Biosensors and Bioelectronics 53 (2014) 257–262

Contents lists available at ScienceDirect

Biosensors and Bioelectronics

journal homepage: www.elsevier.com/locate/bios

# Aptamer-based array electrodes for quantitative interferon-γ detection

Yu Chen *, Tze Sian Pui, Patthara Kongsuphol, Kum Cheong Tang, Sunil K. Arya

*Institute of Microelectronics, A*STAR (Agency for Science, Technology and Research) Singapore, 11 Science Park Road, Singapore Science Park II, Singapore 117685, Singapore*

ARTICLE INFO

*Article history:*
Received 28 July 2013
Received in revised form
12 September 2013
Accepted 13 September 2013
Available online 8 October 2013

*Keywords:*
IFN-γ
Biosensor
Square Wave Voltammetry
Micro-electrode array
Aptamer

ABSTRACT

Present work describes the methylene blue tagged thiolated aptamer-modified gold micro-array based biosensor for specific detection of IFN-γ. The microchips with the microelectrode array were fabricated using standard silicon microfabrication technologies, and modified with methylene blue tagged aptamer using standard gold thiol chemistry. Electrodes were characterized and tested using Cyclic Voltammetric (CV) and Square Wave Voltammetry (SQW) measurements in a standard three-electrode format at room temperature. On an aptamer modified electrode, aptamer density was estimated to be about $4.4 \times 10^{12}$ molecules/cm$^2$. In IFN-γ studies, oxidation peak currents were found to decrease and more than 50% signal suppression was achieved at 500 ng/ml. Further, the magnitude of signal suppression was found to be logarithmically proportional to the IFN-γ in the concentration range of 1–500 ng/ml, with a detection limit of 1.3 ng/ml (i.e. 0.8 fmol in used sample volume of 10 μl). Biosensor showed negligible signal changes (5%) in a very high non-specific protein background, while still able to differentiate target protein IFN-γ at 5 ng/ml. The results indicated that our sensor binds selectively to target molecules, and the non-specific binding where adsorption of BSA protein molecules may be effectively omitted from consideration.



## 1. Introduction

Cytokines, which play a pivotal role in the differentiation, maturation, and activation of various immune cells, are biologically active molecules and an integral part of the immune system. They are prospective biomarkers to monitor disease activity and predict disease severity (Parikh et al., 2005; Dinan et al., 2006; Gambotto et al., 2008). In addition, the manipulation of the cytokines may become potential therapeutic targets for the treatment of infectious diseases, neurological diseases and cancer (Lucey et al., 1996; Wesselingh et al., 1994; Lin and Karin, 2007; Saito et al., 1994) as well as targets for vaccine development (Barouch et al., 1998). Therefore, their detection is of immense diagnostic value.

Interferon gamma (IFN-γ), a 15.5 kDA molecule, is a cytokine capable of activating multiple signal transduction pathways through transcription regulation of immunologically relevant genes. In the family of cytokines, IFN-γ is secreted mainly by macrophages (Okamura et al., 1995). The primary role of IFN-γ is to mediate cellular immune response to viral and mycobacterial infections (Chesler and Reiss, 2002). However, it is also involved in directing several immunoregulatory mechanisms that enhance the cytokine's function (Fruchta et al., 2001; Kukreja et al., 2002). Dysregulations of IFN-γ secretion are implicated in a variety of diseases such as inflammatory bowel disease (IBD) (Rafa et al., 2010), Genital HSV infections (Singh et al., 2003) and Alzheimer's disease (Solerte et al., 2000). Cytokines measured in the blood of dengue patients have revealed significantly increased concentrations of IL-1β, IL-8, TNF-α, IL-6 and IFN-γ (Malavige et al., 2012; Bethell et al., 1998). Of particular interest is IFN-γ, which was suggested as independent predictive markers of dengue severity (Malavige et al., 2012). Compared to other cytokines, which increase with delayed kinetics, IFN-γ is highly expressed early after onset of disease (2–5 d) and is therefore a good predictive marker (Itoh et al., 1998).

Conventionally, cytokines are measured using enzyme-linked immunosorbent assay (ELISA), western blot and biochemical assays on cytokine-sensitive cells. These methods, however, are limited to very low sensitivity and require sample separation, labeling or signal amplification. Detection of cytokines by a capacitance based sensor, field effect transistor sensor and waveguide grating sensor that make use of antibody have been reported (Qureshi et al., 2010; Pui et al., 2011; Luchansky and Bailey, 2010). Although these sensors have high sensitivity, the development of these biosensors requires the use of antibodies, which are expensive and not stable (Liss et al., 2002). Thus there is a scope to develop new methods and platforms for better performance.

Recently, some attentions have been focused on aptamer sensors as new molecular recognition devices (Liss et al., 2002). An aptamer is a nucleic acid macromolecule that binds to a specific target molecule. This type of nucleic acid provides another approach for selective binding to target proteins or enzymes based on their defined tertiary structures. Moreover, as compared with antibodies, aptamers can have similar affinity to their protein

* Corresponding author. Tel.: +65 6770 5693; fax: +65 6773 1914.
*E-mail address:* cheny1@ime.a-star.edu.sg (Y. Chen).

0956-5663/$ - see front matter © 2013 Elsevier B.V. All rights reserved.
http://dx.doi.org/10.1016/j.bios.2013.09.046

targets but are chemically stable, small in size, inexpensive, and much easier to reproduce (Zhou et al., 2010). Therefore, aptamers are suitable to be used as a powerful biological diagnostic tool.

Efforts have been made to achieve the high sensitivity IFN-γ detection by electrochemical methods on aptamer modified gold (Au) electrode. Recently, Liu et al. had demonstrated the proof of concept and feasibility of detecting IFN-γ using redox-labeled aptamer on macro-size electrode (Liu et al., 2011). In their work they used hairpin-like aptamer for detection, which upon unfolding in presence of IFN-γ resulted in decreasing electron transfer from the redox label to the electrode. However, their device, while improving on the existing detection sensitivity, has the following limitations: their device is difficult for large-scale manufacturing by using glass as a substrate. In addition, it is also impossible to integrate *active* electronic circuit underneath the glass substrate to form a system to individually address multiple electrodes.

In this work, we present a low cost and highly sensitive aptamer-based array electrode for detecting IFN-γ. Array of gold electrodes were fabricated on a silicon substrate, with a common photolithography process standardized in large scale production of microelectronics. The advantages of using silicon lie in their potential to integrate *active* electrical components on chip for increased operating speeds, system reliability and equipment density. The approach for immobilizing aptamers against IFN-γ on micro-size electrodes and deploying these sensing surfaces for IFN-γ detection described here will be enhanced in the future to enable high-throughput detections of multiple cytokines arranged into a high-density array.

## 2. Experimental details

### 2.1. Materials and chemicals

Phosphate-buffered saline (PBS), sodium bicarbonate ($NaHCO_3$), 6-mercapto-1-hexanol (MCH), bovine serum albumin (BSA), tris-(2-carboxyethyl) phosphine hydrochloride (TCEP), urea, and DMF were obtained from Sigma Aldrich (USA). Methylene blue (MB), carboxylic acid, succinimidyl ester (NHS) and cell culture medium RPMI 1640 were purchased from Biosearch Technologies (Novato, CA) and VWR respectively. The 34 mer IFN-γ binding aptamer, modified at the 5′-terminus with an amine group for redox probe (MB) conjugation and at the 3′-end with a C6 disulfide linker, was purchased from IDT Technologies (San Diego, DA). Its sequence is as follows: 5′-$NH_2$–$C_6$–GGGGTTGGTTGTGTTGGGTGTTGTGTCCAACCC-$CC_3$–SH-3′. The aptamer stock solution of 34-base oligomers (20 μM) and its aliquot were prepared using PBS buffer (pH 7.4 with 150 mM NaCl). Human recombinant IFN-γ was purchased from R & D systems (Minneapolis, MN). Ag/AgCl solid reference electrode was obtained from A-M system (#550008).

### 2.2. Microchip design and fabrication

The microchips with the microelectrode array were fabricated using standard silicon microfabrication technologies (Ng et al., 2010). Ti/Au (0.1 μm/1.0 μm) layer was deposited onto the 500 nm thick thermal growth oxide layer. Photolithography was used to define the disk electrode layout and the unpatterned metal regions were etched with Au etchant and Ti etchant. Then, the photoresist was stripped off followed by second photolithography to passivate the unpatterned region with $SiO_2$/SiN (0.8 μm/0.2 μm) layers through plasma enhanced chemical vapor deposition (PECVD).

### 2.3. Gold electrodes cleaning

Prior to use, a patterned gold electrode array was washed with IPA, rinsed with distilled water and dried with nitrogen. The chip was then immersed in a piranha solution ($H_2SO_4$/$H_2O_2$, 2/1 ratio) for 5 min and sonicated twice in ultrapure water for 5 min each time. The gold disk working electrodes were then subjected to electrochemical pretreatment in 0.5 M $H_2SO_4$ solution by 100 cyclic scans from −0.35 V to 1.2 V at a scan rate of 2 V/s and 20 cyclic scans from 0.2 V to 1.2 V at a scan rate of 0.1 V/s.

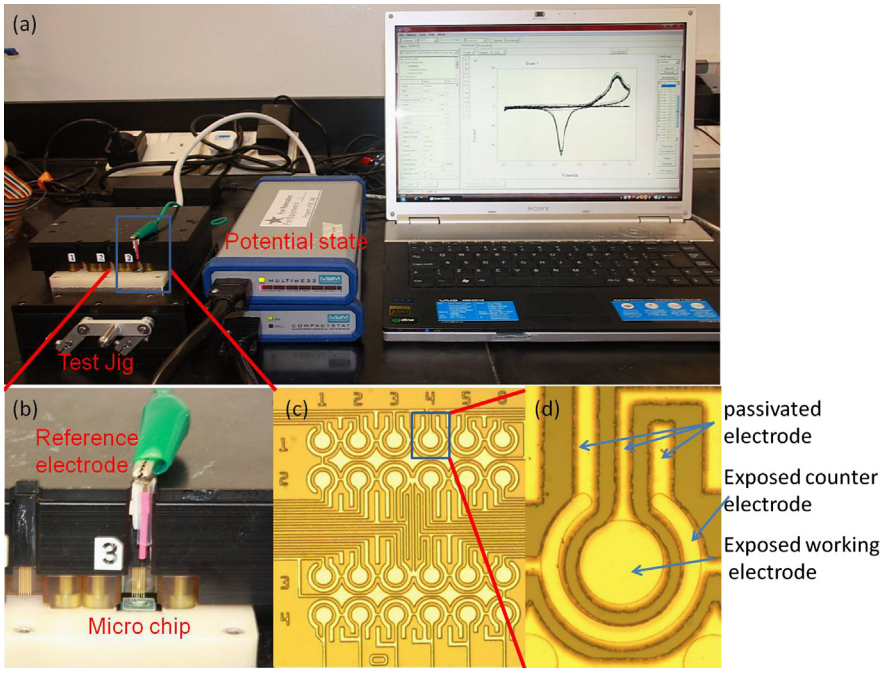


**Fig. 1.** (a) Experimental setup of the measurement including a test jig. (b) Microchip mounted on the testing jig. (c) 24 microelectrode array on a single chip. (d) Au disc working electrode which is surrounded by a horse-shoe shaped counter electrode.

### 2.4. Immobilization of aptamers

A 200 μM MB labeled aptamer solution was reacted with 10 mM TCEP for 2 h at room temperature in a 1:3 (v/v) ratio. The TCEP, a reducing agent, cleaves the disulfide bond on the aptamer, generating a free thiol group to react with gold electrodes to form a self-assembled monolayer (SAM). Phosphate-buffered saline (PBS; 137 mM NaCl, pH 7.4) was used to dilute this reaction solution to a series of concentration (from 0.1 to 5 μM). To immobilize the reduced thiolated aptamer on the electrode array, 20 μl of the diluted solution was transferred into the chamber and subsequently incubated with gold electrode array overnight at 4 °C in dark. After the immobilization, the aptamer-modified chip was rinsed thoroughly with ultrapure water and then treated with 3 mM MCH at room temperature for 1 h. Finally, the chip was rinsed with ultrapure water and blown dry with nitrogen.

### 2.5. System measurement

The experimental setup indicating the basic components of the recording system is shown in Fig. 1a. It consists of a test jig incorporated with 24 probes (spaced evenly at 500 μm), which enables direct electrical connection to the electrode pad on the microchip, and an Ivium Compactstate and MultiWE32 multi-channel potentiostat unit (Ivium Technologies, Netherlands), which controls up to 32 working electrodes that share a common reference electrode (RE) and a common counter electrode. The counter electrode has been designed in such a way that each individual working electrode experiences a similar electrical field during the measurement. The whole recording system is connected to a computer which is equipped with software "IviumSoft" for simultaneous data acquisition of all recording channels.

### 2.6. Electrochemical methods

Cyclic Voltammetric (CV) and Square Wave Voltammetry (SQW) measurements were performed using the MultiWE32 multi-channel potentiostat in a custom-built test cell (Fig. 1a and b). All the electrochemical measurements were performed in a standard three-electrode format at room temperature. The aptamer-modified Au disk electrodes and Au horseshoe shaped electrode patterned on the microchip were acting as working electrodes and counter electrode respectively (Fig. 1c). A sintered Ag/AgCl (A-M system #550008) wire that was immersed in the measurement buffer solution acted as a reference electrode (Fig. 1b). The electrolyte was purged with nitrogen for 10 min prior to measurements to remove the dissolved oxygen. Square wave voltammograms were recorded by applying potential over the range from −0.5 V to 0.2 V, pulse amplitude 50 mV, potential step 5 mV and frequency 1000 Hz. To calibrate the aptamer-modified electrode response, 10 μl of the buffer solution (1 × PBS) added with an increase of IFN-γ was put into the chamber and incubated for 15 min. Peaks height for the methylene blue (MB) reduction was then recorded. The concentration of IFN-γ was quantified by calculating the change of averaged oxidation peak currents over five selected working electrodes $\Delta I$ ($\Delta I = I_o - I$), where $I_o$ and $I$ was the MB oxidation peak current before and after IFN-γ binding interaction, respectively. Detection of IFN-γ in cell culture medium (RPMI) and BSA solution was also carried out.

## 3. Results and discussion

### 3.1. Characterization of the aptamer-modified electrodes

Fig. 1c depicts the optical image of microchip, which consist of 24 small Au disc electrodes and each electrode is 100 μm in diameter. All Au disc electrodes share a common counter electrode, which has been designed in such a way that each individual working electrode experiences similar electrical field during the measurement. The Au disc electrodes are grouped in cluster (12 electrodes each), separated uniformly at 500 μm. Such layout has an advantage for multiplexed sensing as a cluster may serve as one sensing unit for a particular molecular target. Fig. 1d depicts a typical zoom-in optical image of the Au disc working electrode that is surrounded by a horse-shoe shaped counter electrode.

Fig. 2a shows the multiple overlapping of cyclic voltammograms for 12 clean gold working electrodes. The results indicated that our fabrication and cleaning processes produce good, uniformity and reproducibility gold working electrodes. The average reduction peak current was $(2.24 \pm 0.15) \times 10^{-8}$ A, RSD = 7% and average reduction peak potential was (0.680 ± 0.005) V, RSD = 1%. The real working electrode area was estimated from the voltammogram by integration of reduction peak for the charge consumed during the reduction of surface gold oxide (Abad et al., 2002). The average real working electrode area was $(1.46 \times 10^{-4}\ \mathrm{cm}^2)$ and a roughness factor of 1.8 was typically observed.

Fig. 2b (inset) shows that a methylene blue (MB) redox peak pair appears in a cyclic voltammogram of MB tagged aptamer gold

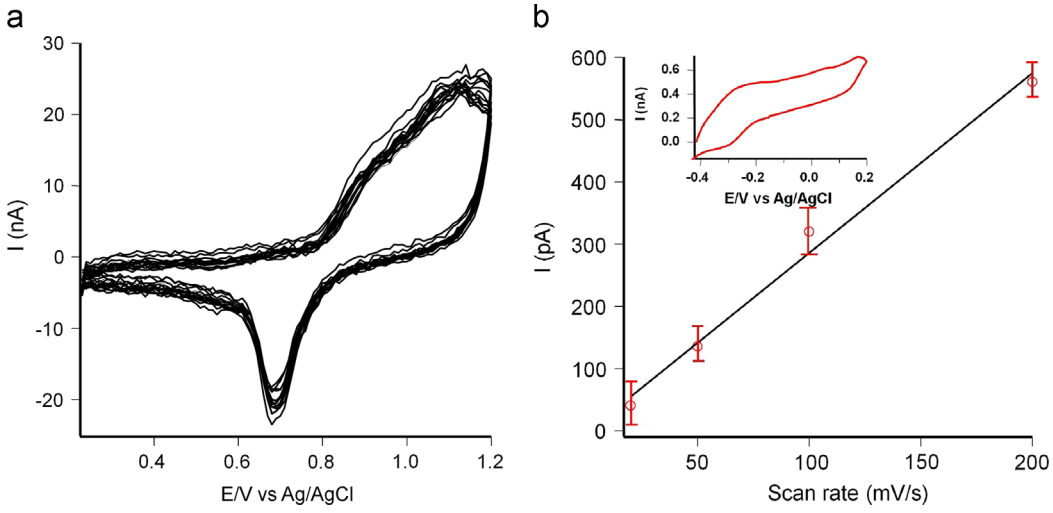


**Fig. 2.** (a) Multiple overlapping of cyclic voltammograms for 12 clean gold working electrodes. (b) Oxidation peak currents versus the scan rate and methylene blue (MB) redox peak pair appears in a cyclic voltammogram of MB tagged aptamer gold working electrode (inset).

working electrode. The formal potential ($E^{o'}$) of the MB, as calculated from the average of reduction and oxidation peak potential, was −0.275 V. This value is close to the typical redox potential of MB reported elsewhere (Rezaei-zarchi et al., 2009). In contrast, gold working electrode modified with MCH or MB-free aptamer does not show a cyclic voltammetry peak in the range of −0.4 to 0.2 V (data not shown). These measurements indicate clearly that our functionalization step to immobilize MB tagged aptamer onto gold electrode is successful, and MB labeled at the terminal of aptamer allows efficient electron transfer. To further confirm that MB is tagged on the aptamer is confined at the electrode surface, we also modulate the scan rate of the cyclic voltammetries. Fig. 2b shows that oxidation peak currents are directly proportional to the scan rate, which is a typical surface-controlled electrode process (Fan et al., 2003).

### 3.2. Detection of IFN-γ using aptamer modified electrode

To detect IFN-γ binding event, we used square wave voltammetry to monitor faradaic current from the MB-tagged aptamer. In the absence of IFN-γ, the MB-tagged aptamer folds into a hairpin structure where the redox label is in a close proximity to the electrode surface (Fig. 3a). In this case, a high electron-transfer rate for redox reaction of MB is obtained. Upon binding of IFN-γ, the aptamer is unfolded to form a protein–aptamer complex (Fig. 3b). This structure enables MB at the terminal of aptamer to be pushed away from the electrode, resulting in an inhibiting of electron transfer reaction. Fig. 3c confirms the feasibility of the present electrochemical aptamer-based sensor. The SQW peak appearing at −0.25 V (redox potential of MB) is significantly reduced upon addition of target IFN-γ in PBS (0.5 ng/ml). The magnitude of signal suppression is enhanced over time and the sensor achieves a signal loss about 25% of its initial value after 15 min incubation. In the following experiments, a fixed 15 min incubation time was then chosen for binding of target protein to aptamer-modified electrode.

### 3.3. Influence of aptamer surface density on sensor response

It is apparent that the limit of aptamer based sensor performance is also dependent on the density of aptamer on the electrode surface (Ricci et al., 2007). We have modified electrode with aptamer using a concentration range from 0.2 μM to 5 μM. Before SQW measurement, aptamer modified electrodes were equilibrated by incubating in PBS buffer for 30 min. Then, SQW measurement was performed followed by challenging the aptamer modified electrode with 200 ng/ml IFN-γ. The difference in faradaic current before and after the target binding divided by the initial faradiac current was taken as signal suppression, an indicator of sensor performance. The largest signal suppression shows the most sensitive sensor. We can reproduce sensors of aptamer densities from $4.4\times10^{12}$ to $8.95\times10^{12}$ molecules/cm$^2$ (assuming one MB molecule was conjugated to one aptamer and perfect electron transfer efficiency). Fig. 3d shows that low aptamer density produces the largest signal suppression of 38 ± 5%, which is 2.4 times more sensitive than the electrode modified with the highest aptamer density. Such magnitude of signal suppression

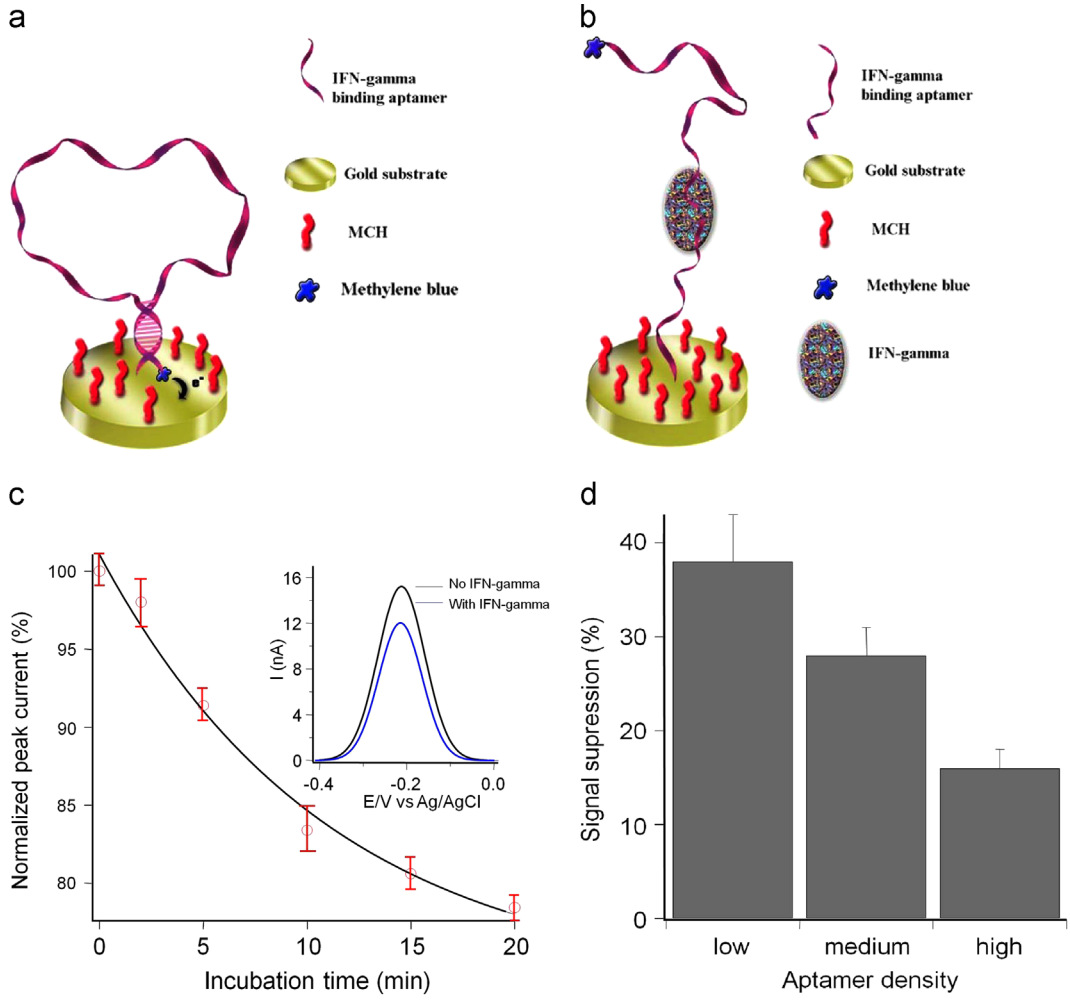


**Fig. 3.** Demonstration of the MB-tagged aptamer modified electrode (a) before IFN-γ binding, and (b) after IFN-γ binding. (c) The magnitude of signal (peak current) versus incubation time. The IFN-γ concentration is 5 ng/ml. (d) Signal suppression versus aptamer density on the electrode. The IFN-γ concentration is 200 ng/ml.

influenced by the density of aptamer is in agreement with the results reported using a larger gold working electrode (diameter is 1.6 mm) (Liu et al., 2011).

### 3.4. Sensitivity and specificity test

To calibrate the sensor responses, the buffer solution mixed with IFN-γ in the range from 1 to 500 ng/ml was added onto the aptamer modified electrode (aptamer density is about $4.4 \times 10^{12}$ molecules/$cm^2$) while SQW measurement was performed at 1000 Hz frequency, 50 mV pulse amplitude, and with 5 mV potential step over a potential range from −0.5 to 0.2 V. As expected, the oxidation peak currents decreased and more than 50% signal suppression was achieved at 500 ng/ml (Fig. 4). The magnitude of signal suppression was logarithmically proportional to the IFN-γ concentration: $\Delta I_n = -15.35 \log n - 8.39$, where $\Delta I_n$ is the percentage change of the current due to the IFN-γ concentration $n$. The standard deviation of the current change is around 2.2%. The detection limit is estimated to be 1.3 ng/ml, where the current change is −6.6%, which is three times of the standard deviation. This is comparable to what has been reported about label free-electrochemical sensors (Liu et al., 2011). Importantly, we employ a finger-prick sample volume of 10 μl, equating to an absolute detection limit of 0.8 fmol. Compared to the single large electrode sensor used by Liu et al., our chip is a multi-electrode array that offers great potential for multiplexing and the chip can be packaging for on-site measurement.

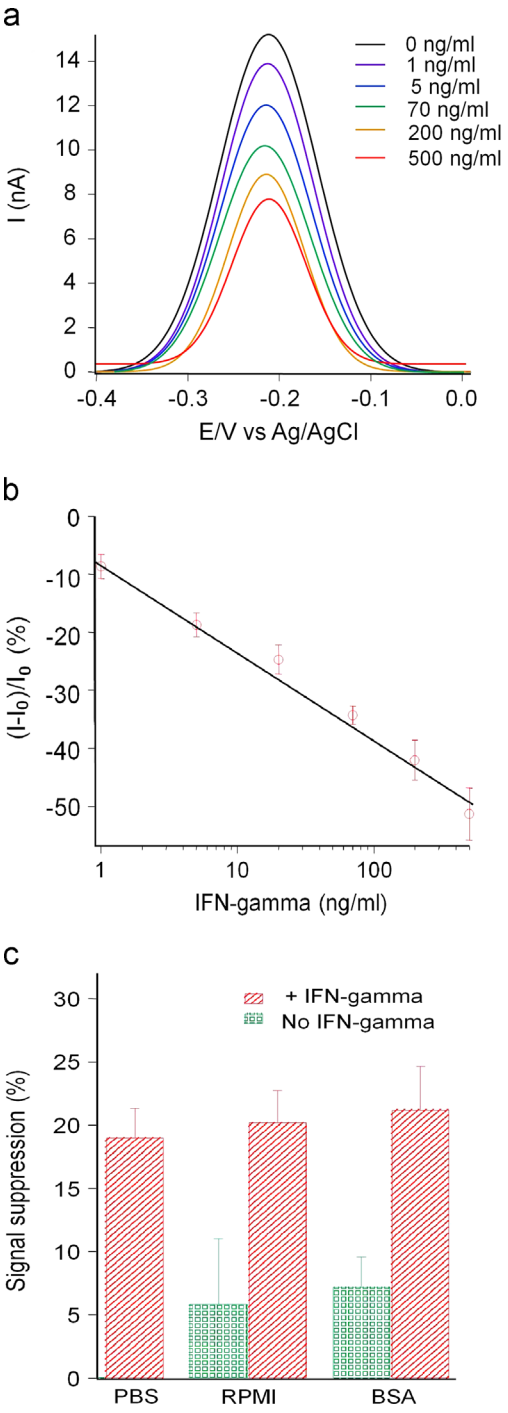


**Fig. 4.** (a) Cyclic voltammograms of the device at different IFN-γ concentration. (b) Signal change versus IFN-γ concentration. (c) The signal suppression at different media with and without IFN-γ binding. The data points were averaged from 5 working electrodes.

In order to quantify any background effect due to nonspecific binding of proteins to the modified electrodes, a control experiment was carried out with a device prepared in the same way as described in the method section. We investigated the electrode response to cell culture medium and bovine serum albumin, BSA (100 μg/ml in RPMI medium) with and without a target protein. Fig. 4c shows negligible signal changes (5%) in a very high non-specific protein background while still able to differentiate target protein IFN-γ at 5 ng/ml. A distinctive 20% signal suppression is observed. The results indicated that our sensor is selective to target molecules and the non-specific binding and adsorption of BSA protein molecules may effectively be omitted from consideration.

## 4. Conclusion

In summary, we have demonstrated a low cost, aptamer-based array electrode on silicon substrate for specific detection of IFN-γ. The advantages of using silicon lie in their potential to integrate *active* electrical components on chip for increased operating speeds, system reliability and equipment density. IFN-γ is of particular importance after infections since it orchestrates the regulation and termination of an inflammatory response. Using this aptamer-based electrode, a linear relationship was found between the reductions current of MB and logarithmic value of the IFN-γ concentration. Our biosensor is able to detect IFN-γ in a concentration range of 1–500 ng/ml, with detection limit of 1.3 ng/ml. This biosensor promises novel applications for fundamental cell studies, diagnosis and therapy monitoring. The measurements in clinic samples as well as the test of multiple cytokines simultaneously are in the process of studying.

## Acknowledgment

The authors would like to acknowledge The Agency for Science, Technology and Research (A*STAR) Joint Council Office Grant ("JCO Grant") Microdevice for Quantitative detection of Cell type-specific Cytokines for Biomarker Validation and Clinical Research (11/03/FG/07/03).

## References

Abad, J., Velez, M., Santamaria, C., Guisan, J., Matheus, P., Vazquez, L., Gazaryan, I., Gorton, L., Gibson, T., Fernandez, V., 2002. Journal of the American Chemical Society 124, 12845–12853.
Barouch, D.H., Santra, S., Steenbeke, T.D., et al., 1998. Journal of Immunology 161 (4), 1875–1882.
Bethell, D.B., Flobbe, K., Phuong, C.X.T., Day, N.P.J., Phuong, P.T., Buurman, W.A., Cardosa, M.J., White, N.J., Kwiatkowski, D., 1998. The Journal of Infectious Diseases 177 (3), 778–782.

Chesler, D.A., Reiss, C.S., 2002. Cytokine Growth Factor Review 13 (6), 441–454.
Dinan, T.G., Quigley, E.M.M., Ahmed, S.M.M., et al., 2006. Gastroenterology 130 (2), 304–311.
Fan, C., Plaxco, K.W., Heeger, A.J., 2003. Proceedings of the National Academy of Sciences 100 (6), 9134–9137.
Fruchta, D.M., Fukaob, T., Bogdanc, C., Schindlerc, H., O'Sheaa, J.J., Koyasub, S., 2001. Trends in Immunology 22 (10), 556–560.
Gambotto, A., Barratt-Boyes, S.M., de Jong, M.D., Neumann, G., Kawaoka, Y., 2008. The Lancet 371 (9622), 1464–1475.
Itoh, M., Yano, A., Xie, Q., Iwahashi, K., Takeuchi, Y., Meroni, P.L., Nicoletti, F., 1998. Clinical and Experimental Immunology 111 (3), 513–520.
Kukreja, A., Cost, G., Marker, J., Zhang, C., Sun, Z., Lin-Su, K., et al., 2002. The Journal of Clinical Investigation 109 (1), 131–140.
Lin, W., Karin, M., 2007. Journal of Clinical investigation 117 (5), 1175–1183.
Liss, M., Petersen, B., Wolf, H., et al., 2002. Analytical Chemistry 74 (17), 4488–4495.
Liu, Y., Yan, J., Howland, M.C., Kwa, T., Revzin, A., 2011. Analytical Chemistry 83 (21), 8286–8292.
Lucey, D.R., Clerici, M., Shearer, G.M., 1996. Clinical Microbiology Reviews 9 (4), 532–562.
Luchansky, M., Bailey, R., 2010. Analytical Chemistry 82 (5), 1975–1981.
Malavige, G.N., Huang, L.C., Salimi, M., Gomes, L., Jayaratne, S.D., Ogg, G.S., 2012. PLOS ONE 7 (11), 50387.
Ng, S.Y., Reboud, J., Wang, K.Y.P., Tang, K.C., Zhang, L., Wong, P., Moe, K.T., Shim, W., Chen, Y., 2010. Biosensors and Bioelectronics 25, 1095–1101.
Okamura, H., Tsutsui, H., Komatsu, T., et al., 1995. Nature 378 (6552), 88–91.
Parikh, C.R., Abraham, E., Ancukiewicz, M., Edelstein, C.L., 2005. Journal of the American Society of Nephrology 16, 3046–3052.
Pui, T.S., Agarwal, A., Ye, F., et al., 2011. Biosensors and Bioelectronics 26 (5), 2746–2750.
Qureshi, A., Niazi, J.H., Kallempudi, S., Gurbuz, Y., 2010. Biosensors and Bioelectronics 25 (10), 2318–2323.
Ricci, F., Volpe, G., Micheli, L., Palleschi, G., 2007. Analytica Chimica Acta 605 (2), 111–129.
Rafa, H., Amri, M., Saoula, H., Belkhelfa, M., Medjeber, O., Boutaleb, A., Aftis, S., Nakmouche, M., Touil-Boukoffa, C., 2010. Journal of Interferon and Cytokine Research 30 (9), 691–697.
Rezaei-zarchi, S., Javed, A., Mirjalili, H., Abarghouei, H.B., Hashemizadeh, S.A., 2009. Turkish Journal of Chemistry 33, 411–420.
Saito, S., Bannerji, R., Gansbacher, B., et al., 1994. Cancer Research 54 (13), 3516–3520.
Singh, R., Kumar, A., Creepy, W.D., Ruben, M., Giulivi, A., Diaz-Mitoma, F., 2003. Clinical and Experimental Immunology 133 (1), 97–107.
Solerte, S.B., Cravello, L., Ferrari, E., Fioravanti, M., 2000. Annals of the New York Academy of Science 917, 331–340.
Wesselingh, S.L., GLASS, J., Mcarthur, J.C., et al., 1994. Advances in Neuroimmunology 4 (3), 199–206.
Zhou, J., Battig, M.R., Wang, Y., 2010. Analytical and Bioanalytical Chemistry 398 (6), 2471–2480.